Available online at www.sciencedirect.com
SCIENCE DIRECT®
Dyes and Pigments 71 (2006) 178–187
DYES and PIGMENTS
www.elsevier.com/locate/dyepig

3,4,9,10-Perylenetetracarboxylic acid derivatives and their photophysical properties

V.J. Sapagovas [a,*], V. Gaidelis [b], V. Kovalevskij [c], A. Undzenas [c]

[a] Vilnius University, Department of Organic Chemistry, Naugarduko 24, LT-03225 Vilnius, Lithuania
[b] Vilnius University, Department of Solid State Electronics, Sauletekio al. 9, LT-10222 Vilnius, Lithuania
[c] Institute of Physics, Savanoriu pr. 231, LT-02300 Vilnius, Lithuania

Received 28 January 2005; received in revised form 29 April 2005; accepted 23 June 2005
Available online 18 August 2005

Abstract

The aggregation in solutions of perylene pigments *N*,*N*′-diphenyl-, *N*,*N*′-dibenzyl- and *N*,*N*′-diphenethyl-3,4,9,10-perylenetetracarboxylic acid diimides in chloroform and dimethylsulfoxide solutions was studied. UV/Vis absorption spectra at different concentrations were recorded and it was shown that pigment molecules underwent aggregation to form dimers at larger solution concentrations. Monomer and dimer spectra of the pigments as well as aggregation degrees *n* and equilibrium constants *K* were calculated employing concentration-dependent measurement data of pigment solutions. Single- and dual-layered photoreceptors employing 3,4,9,10-perylenetetracarboxylic acid derivatives as charge-generating materials were prepared and their xerographic characteristics were measured. Incorporating a charge blocking layer into the dual-layered photoreceptors led to the enhanced photosensitivity, but a faster dark decay of the initial surface potential as well as slightly inferior homogeneity of the system was also observed.

Keywords: Perylenes; Pigments; Heterocycles; Aggregation; Xerography; Photoreceptors

1. Introduction

At present organic materials with highly developed conjugated π-electronic systems are widely used in various optoelectronic devices, in most cases replacing inorganic semiconductors. Their advantages over inorganic counterparts are low toxicity, technological merits in producing photoconductive compositions and the ease of fabrication of large area devices [1,2]. One of the promising classes among organic substances that have found the application in fabricating organic photoreceptors are derivatives of 3,4,9,10-perylenetetracarboxylic acid. They are widely used in electrophotographic photoreceptors [1,2], light-emitting diodes [3,4], field-effect transistors [5], solar cells [6] and other optoelectronic and photonic devices. One of the principal applications of photosensitive perylene pigments is their use in organic electrophotography as charge-generating and electron-transporting materials.

The high sensitivity to radiation in UV/Vis/near IR spectral regions is an indispensable requirement for organic photoconductors. This wavelength range includes the entire visible region needed for copier and solar cell applications as well as a 750–850-nm region for digital copier and laser printer applications. The only limitation of photoconductive perylene pigments is their low spectral sensitivity in the near IR region. Some pigments, like 3,4,9,10-perylenetetracarboxylic acid bisbenzimidazole, already possess sufficient sensitivity up to 750 nm wavelength, therefore, technological attempts of reaching the 780 nm limit (the radiation is emitted by

* Corresponding author. Tel.: +370 5 2336508; fax: +370 5 2330987.
E-mail address: vytenis.sapagovas@chf.vu.lt (V.J. Sapagovas).

0143-7208/$ - see front matter © 2005 Elsevier Ltd. All rights reserved.
doi:10.1016/j.dyepig.2005.06.012

widely used GaAs diode lasers) would permit the use of the pigment as a charge-generating material in commercial digital electrophotography devices.

Although UV/Vis solution absorption of *N*,*N*′-dialkyl-(or *N*,*N*′-diaryl)-3,4,9,10-perylenetetracarboxylic acid diimides is independent of the substituents at the nitrogen atoms, situation is different for solid-state samples. Basically, solid-phase absorption peaks are broader and bathochromically shifted due to strong intermolecular π–π interactions. The magnitude of the red shift is related to the crystal structure and strongly depends on the substituents at the nitrogen atoms [7,8]. When substituent conformation in the solid-state favors the strong overlap of π systems of neighboring molecules, the absorption maximum is at >600 nm resulting in the black color of the crystal (e.g., R = C_3H_7, $CH_2CH_2C_6H_5$). When substituents hinder the overlap and weak intermolecular interaction is observed, the absorption maximum is in the range of 550–570 nm resulting in the red color (e.g., R = CH_3, C_5H_{11}). Some pigments with the intermediate overlap absorb at 570–600 nm and possess red-maroon or red-violet color (e.g., R = $CH_2C_6H_5$, C_4H_9). No direct correlation between the structure of the substituent and the color of the crystal could be made [9,10]. However, even the UV/Vis absorption of the solution changes depending on concentration. The aggregation to dimers [11] or maybe even larger aggregates [12] at higher concentrations is reported. There are indications that derivatives of perylenetetracarboxylic acid favor charge transfer due to large intermolecular coupling, and this may lead to the formation of charge transfer excitons [13].

In the present work, the purposeful synthesis of several particular derivatives of 3,4,9,10-perylenetetracarboxylic with substituents at the nitrogen atom was performed. Their UV/Vis absorption in diluted solution and aggregation process at various concentrations were also carefully investigated in detail. Moreover, the comparison between solution absorption spectra and absorption of these pigments dispersed in a polyvinylbutyral polymeric film was performed in order to elucidate the influence of the aggregation effect that is very sensitive to substituents at the nitrogen atoms, on the photoconductive properties of these materials. Finally, a comparison of electrophotographic properties of single- and dual-layered photoreceptors containing 3,4,9,10-perylenetetracarboxylic acid derivatives has been performed in order to clarify general guides for obtaining an efficient charge-generating and photoconducting material.

2. Experimental

UV/Vis absorption spectra were recorded with a UV/Vis Spectrometer Perkin Elmer Lambda 20. All measurements were performed at room temperature.

2.1. Synthesis and purification of pigments *1a–c* and *2*

3,4,9,10-Perylenetetracarboxylic acid dianhydride and corresponding amine, diamine or amine hydrochloride in the molar ratio 1:3 were heated in quinoline under nitrogen atmosphere at 180 °C for 4–6 h. The reaction mixture was washed several times with methanol to remove quinoline, with KOH methanolic solution to remove unreacted anhydride, then again with methanol, with water and, finally, dried. Pigments were purified by precipitating their solutions in a concentrated sulfuric acid into water. The synthesis and purification procedures were described in detail in our previous paper [14]. Synthesized perylenetetracarboxylic acid diimides are thermally very stable. They undergo neither melting nor decomposition at temperatures up to 500 °C. Therefore, their melting points cannot be determined.

2.2. Sample preparation for solid-state absorption measurements

Forty milligrams of pigment, 1.5 mL of 40 mg mL^{-1} polyvinylbutyral (Aldrich, M_W 90,000–120,000) solution in 1-butanol and 3 mL of 1-butanol were placed in a stainless steel container filled with 4 mm diameter stainless steel balls and dispersed for 15–20 h. After dispersing, a thin film of the dispersion was coated on a glass plate and dried at room temperature. Colors of the films obtained were red for diimide **1a**, red-maroon for diimide **1b** and black for diimide **1c**.

2.3. Sample preparation for solution absorption measurements

About 100–200 mg L^{-1} ($\sim 10^{-4}$ mol L^{-1}) solutions in dimethylsulfoxide (DMSO) and chloroform were prepared after dispersing pigments in the ultrasound bath for 4–15 h (until all of the pigment dissolved). Other solutions were prepared by diluting the initial solution. At least three different initial solutions were prepared for every pigment–solvent combination in order to minimize experimental errors.

2.4. Photoreceptor preparation and xerographic measurements

For manufacturing pigment-containing xerographic photoreceptors the following materials were used. Polyvinylbutyral (M_w = 70,000–100,000, Aldrich), Polycarbonate Iupilon Z200 (Mitsubishi Engineering-Plastics Corp.), ELA3011 (9-ethylcarbazole-3-aldehyde-*N*,*N*-diphenylhydrazone, H.W. Sands Corp.), ELA4021 (*N*,*N*′-bis-(3-methylphenyl)-*N*,*N*′-bis-(phenyl)-benzidine,

H.W. Sands Corp.), and ST-917 ([2-(4-(1-methylethyl)-phenyl)-6-phenyl-4*H*-thiopyran-4-ylidene]-propanedinitril-1,1-dioxide, SynTec GmbH). The materials as well as conventional organic solvents were used as received without further purification. Chemical structures of materials used are presented in Figs. 1 and 6.

Perylene pigment dispersions in tetrahydrofuran (THF) were prepared by dispersing the pigment and solvent mixture in the shaking apparatus (shaking frequency 2.25 s^{-1}) for 12 h and afterwards dispersing it with polyvinylbutyral and THF in the vibration mill (shaking frequency 10 s^{-1}) for 3 h. The layer thickness was determined using a mechanical micrometer thickness gauge. All the layers were coated using the dip coating technique.

Single-layered photoreceptors consisted of a blocking sublayer and a photosensitive layer coated onto an aluminum precoated polyester film. The solution of methylmethacrylate and methacrylic acid copolymer (MKM) in a 1:1 acetone and water mixture was used for preparing the blocking sublayer. The thickness of the sublayer was ~0.5 μm. The ~12–15 μm-thick photosensitive layer, containing the perylene pigment, PVB, ELA3011 and ST-917 (their dispersion in THF, mass ratio 1:4:16:8) was overcoated on the blocking sublayer.

Dual-layered photoreceptors consisted of an aluminum precoated polyester substrate, a ~0.5-μm-thick charge-generating layer (CGL) and a ~8–10-μm-thick charge-transporting layer (CTL). The CGL was manufactured employing the dispersion of the perylene pigment and polyvinylbutyral (mass ratio 4:1, dispersion in THF, 0.5 or 1 mol% of ELA4021 may be introduced). ELA3011 and polyvinylbutyral (mass ratio 1:1) or ELA4021 and polycarbonate (PC) (mass ratio 1:1) solutions in THF were used for the coating of CTL. In some cases ~0.5 μm-thick MKM charge blocking layer was introduced between the Al substrate and the CGL.

For electrophotographic measurements a photoreceptor is first charged by a scorotron with a negative potential, and the electric field strength inside photoreceptors was restricted to 50–60 V μm^{-1}. Then the time dependence of the potential discharge $U(t)$ is recorded by exposing the sample to the light at the selected wavelengths λ. An electrometer is calibrated before measurements connecting a voltage source to the conductive substrate of the photoreceptor. The probe above the photoreceptor vibrates with a 0.5-kHz frequency. The signal from the probe is passed to a synchrodetector, connected to a digital oscilloscope and a personal computer with a PCI data acquisition board KPCI-3101-4 (Keithley).

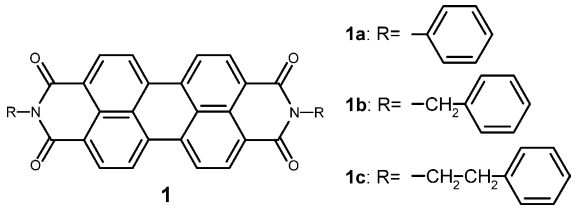

Fig. 1. Chemical structures of perylenetetracarboxylic acid derivatives: **1a** – *N*,*N*′-diphenyl-3,4,9,10-perylenetetracarboxylic diimide, **1b** – *N*,*N*′-dibenzyl-3,4,9,10-perylenetetracarboxylic diimide, **1c** – *N*,*N*′-diphenethyl-3,4,9,10-perylenetetracarboxylic diimide.

The xenon lamp, a diffraction monochromator MDR-2, filters and a photo shutter were used for illumination of the layer. The constant intensity of the light ($I = 10^{17}$ quanta/s m^2) is adjusted by the collimator of the monochromator and measured by a photodiode. All electrophotographic experiments were carried out at room temperature.

The spectral photosensitivity, which is inversely proportional to the energy required to photodischarge half of the initial potential U_0, was calculated using the expression $S_{1/2}\lambda = \lambda/(chIt_{1/2})$, where c is the light speed in the vacuum, h the Planck constant, I the intensity of light, and $t_{1/2}$ is the potential half-decay time (time, when the initial potential reaches $U_0/2$). The residual potential U_R was determined by the photoreceptor potential at time $t = 10t_{1/2}$, i.e., $U_R = U(t = 10t_{1/2})$. The detailed description of xerographic parameters and their measurement may be found in reviews [1,2].

3. Results and discussion

The solutions of synthesized perylene pigments *N*,*N*′-diphenyl- (**1a**), *N*,*N*′-dibenzyl- (**1b**) and *N*,*N*′-diphenethyl- (**1c**) 3,4,9,10-perylenetetracarboxylic diimides (Fig. 1) in chloroform and dimethylsulfoxide (DMSO) were investigated. Although all the three compounds are homologous and possess very similar chemical structure (in **1a** phenyl substituents are attached directly to nitrogen atoms while in **1b** and **1c** phenyls are separated from nitrogens with one and two CH_2 groups, respectively), their color in the solid-state differs significantly [9,10]. Therefore, the variation in intermolecular interactions but not the chemical structure may be the reason of different optical properties in the solid-state as well as in concentrated solutions.

A very low solubility of perylenetetracarboxylic acid derivatives is the main difficulty in obtaining UV/Vis absorption spectra in solution. However, for these derivatives it is possible to prepare ~100–200 mg L^{-1} (~10^{-4} mol L^{-1}) concentration solutions in DMSO and chloroform after dispersing pigments in the ultrasound bath for up to 15 h.

As reported earlier [14], the shape of the absorption spectrum is concentration dependent. For example, dibenzylimide **1b** in DMSO shows monomeric π–π^* transition band at 529 nm with a characteristic vibronic structure. The first absorption maximum at 529 nm represents a lowest energy transition from the ground state (zero vibrational level) to the first excited state,

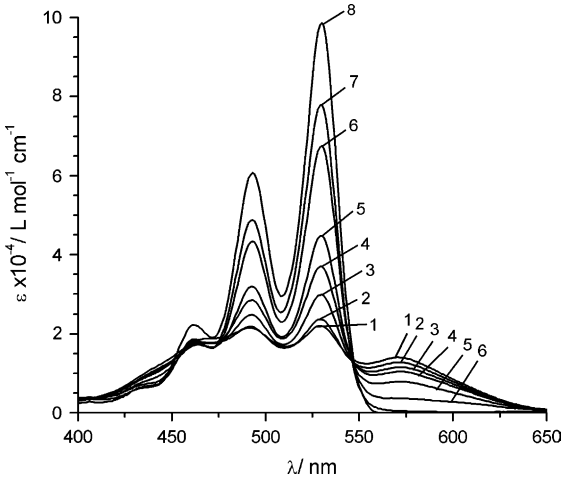

Fig. 2. Absorption spectra of dibenzylimide **1b** solutions in DMSO at various concentrations (1 − $c = 1.39 \times 10^{-4}$, 2 − 6.19×10^{-5}, 3 − 2.23×10^{-5}, 4 − 1.34×10^{-5}, 5 − 8.01×10^{-6}, 6 − 2.89×10^{-6}, 7 − 1.02×10^{-6}, 8 − 2.05×10^{-7} mol L^{-1}).

while three smaller subsequent maxima at 493, 463 and 439 nm correspond to transitions to the various excited vibrational levels of the first electronic excited state, usually marked as the $0 \rightarrow n$ [12,14]. Intensities of these peaks decrease at higher concentrations, while a broad peak due to dimer or larger aggregate at 571 nm appears and its intensity increases with the pigments concentration. The concentration dependence of absorption spectra of dibenzylimide **1b** in DMSO solutions is presented in Fig. 2.

The presence of isosbestic points (the most easily observed one is at 547 nm) in the spectra indicates that only two types of particles: monomers and most probably dimers exist in the solution. The equilibrium between monomer M and n-mer D is characterized by the equilibrium constant K:

$$K = \frac{[D]}{[M]^n}, \tag{1}$$

where n indicates the aggregation degree, e.g., 2 for a dimer. The material balance may be presented as follows:

$$c = [M] + n[D]. \tag{2}$$

This equation relates the concentrations of the monomer and n-mer with the overall concentration c of the pigment.

The fraction of the monomer f_m indicates the ratio of the monomer with the overall concentration, with limiting values zero (pure n-mer) and unity (pure monomer):

$$f_m = \frac{[M]}{c}. \tag{3}$$

It is possible to calculate pure monomer and dimer spectra from absorption spectra of different concentration solutions. Such examples are presented in the literature, e.g., for *N*,*N*′-diglycyl-3,4,9,10-perylenetetracarboxylic diimide dipotassium salt in aqueous solutions [15], or for other pigments such as methylene blue [16] and cyanine dyes [17]. The basis of this method is the calculation of monomer fractions at different concentrations, using the extrapolation to zero and infinite pigment concentrations. After obtaining the values of monomer fractions, it is simple to obtain pure monomer and pure dimer spectra from several spectra of the solution at different concentrations. Such calculations were performed with the solutions of diimides **1a–c** in DMSO and chloroform. The detailed description of the calculations is presented in Appendix 1.

The values of n, log K as well as calculated absorption maxima wavelengths with corresponding extinction coefficients of monomers and dimers are presented in Table 1. Calculated monomer and dimer spectra as well as absorption spectra of the concentrated solution and spectra of the pigments dispersed in the polyvinylbutyral film are presented in Figs. 3–5.

Several regularities may be observed in the obtained data. The obtained values of aggregation degrees $n \approx 2.2$ correspond to the situation when the dimer formation is more preferable (where n must be 2). The possible reasons for the difference may be caused by curve fitting errors, some experimental errors related to very low pigment concentrations, or by solvation effects. But the most preferable reason is the formation of higher order aggregates, maybe even colloidal particles, especially at very high pigment concentrations. The

Table 1
Data of calculated dimer and monomer spectra

Compound	Solvent	n	log K	λ_m (ε_m)	λ_{1d} ($\varepsilon_{1d}/2$)	λ_{2d} ($\varepsilon_{2d}/2$)
1a	DMSO	2.46 ± 0.19	6.58 ± 0.95	528 (90,300)	511 (19,500)	560 (14,100)
	$CHCl_3$	2.23 ± 0.30	5.34 ± 1.54	527 (93,400)	484 (5500)	578 (5800)
1b	DMSO	2.21 ± 0.09	6.60 ± 0.52	530 (94,700)	472 (18,800)	571 (15,300)
	$CHCl_3$	2.20 ± 0.13	5.41 ± 0.67	528 (98,000)	469 (15,200)	602 (15,500)
1c	DMSO	2.27 ± 0.07	7.65 ± 0.46	528 (83,000)	466 (9600)	599 (12,600)
	$CHCl_3$	2.24 ± 0.13	6.01 ± 0.68	526 (83,800)	473 (13,500)	616 (19,400)

n − Calculated aggregation degree; log K − equilibrium constant (L mol^{-1}) logarithm; λ_m − monomer, λ_{1d} and λ_{2d} − dimer calculated absorption maxima wavelengths (nm), ε values (L mol^{-1} cm^{-1}) are given in parentheses (ε_m for monomer, $\varepsilon_d/2$ for dimer).

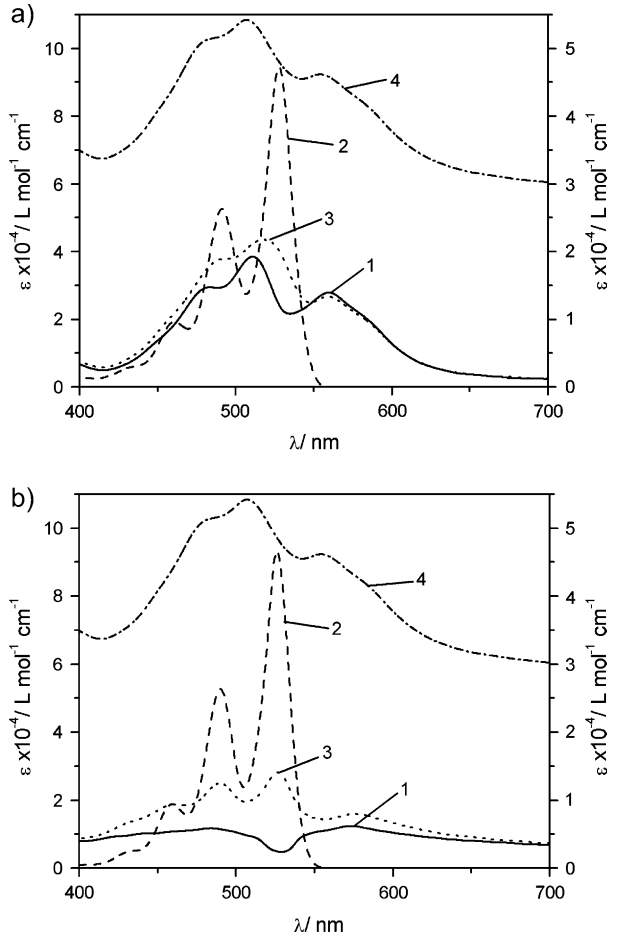

Fig. 3. Absorption spectra of diphenylimide **1a** in (a) DMSO and (b) $CHCl_3$. Calculated dimer (1, solid line, scale on the right axis), calculated monomer (2, dashed line, scale on the left axis), concentrated solution (4.9×10^{-4} mol L^{-1} in DMSO and 4.2×10^{-4} mol L^{-1} in $CHCl_3$, 3, dotted line, scale on the right axis) absorption spectra and absorption spectrum of **1a** dispersed in a polyvinylbutyral film (4, dashed-dotted line, scale in arb.u.).

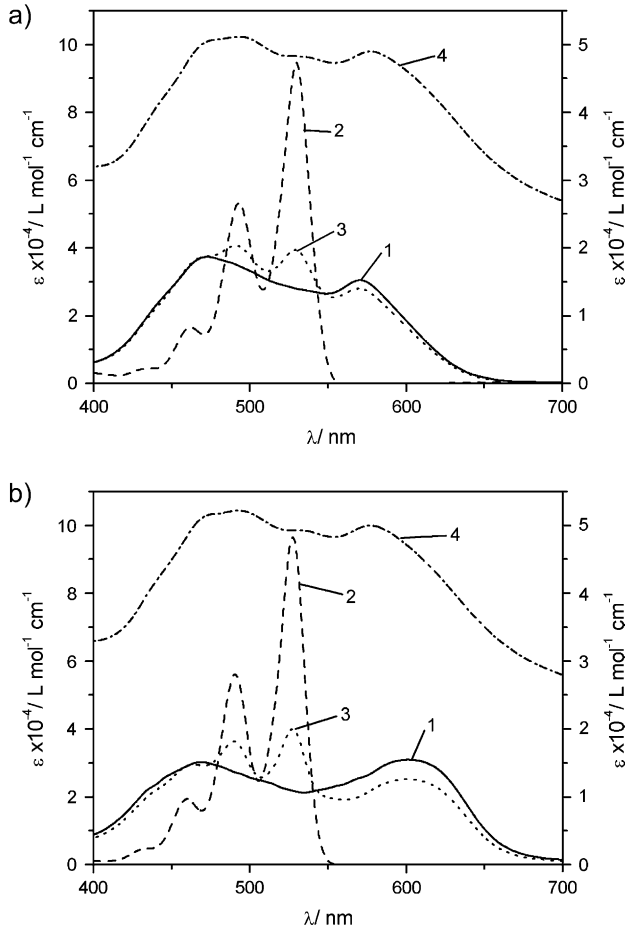

Fig. 4. Absorption spectra of dibenzylimide **1b** in (a) DMSO and (b) $CHCl_3$. Calculated dimer (1, solid line, scale on the right axis), calculated monomer (2, dashed line, scale on the left axis), the concentrated solution (3.9×10^{-4} mol L^{-1} in DMSO and 4.3×10^{-4} mol L^{-1} in $CHCl_3$, 3, dotted line, scale on the right axis) absorption spectra and absorption spectrum of **1b** dispersed in a polyvinylbutyral film (4, dashed-dotted line, scale in arb.u.).

calculated monomer spectra are almost identical to the low concentration ($\leq 10^{-6}$ mol L^{-1}) solution spectra. Two broad peaks at shorter and longer wavelengths relative to the monomeric lowest energy transition appear in the calculated spectra of the dimer. The observed splitting of the spectra may be caused by excitonic coupling in a dimeric aggregate which is similar to Davydov splitting in molecular crystals. Absorption spectra of the pigments dispersed in the polymeric film are very similar to the spectra of the concentrated solutions in DMSO for all pigments. The absorption of the dimer or similar aggregate is also observed in the absorption spectra of the pigment in polyvinylbutyral film, as well as traces of monomeric absorption. The values of the maximum extinction coefficients ε_{max} for the dimers are about 5–6 times smaller as compared to that of the monomer ($\varepsilon_d/2$ is used instead of ε_d, because it corresponds to the same amount of the pigment). The only exception is diphenylimide **1a** dissolved in chloroform, since ε_d for the dimer in this case is much smaller than in other cases. The weak intermolecular interaction strength and a very low solubility may be the reason, that not the proper solution, but some dispersion was formed at higher concentrations in this case, thus decreasing monomer absorption.

A bathochromic shift is observed for the longest wavelength maximum in the dimer spectra in chloroform as opposed to more polar DMSO. This indicates that the excited state of the dimer is less polar than its ground state. The aggregation to dimers is stronger in DMSO than in chloroform for all the three compounds (the values of K are higher). Because DMSO is much polar solvent than chloroform, which implies that the dimeric state is more polar than the monomeric one. Probably, the charge transfer, occurring during the dimerization process, increases the polarity of the dimer state.

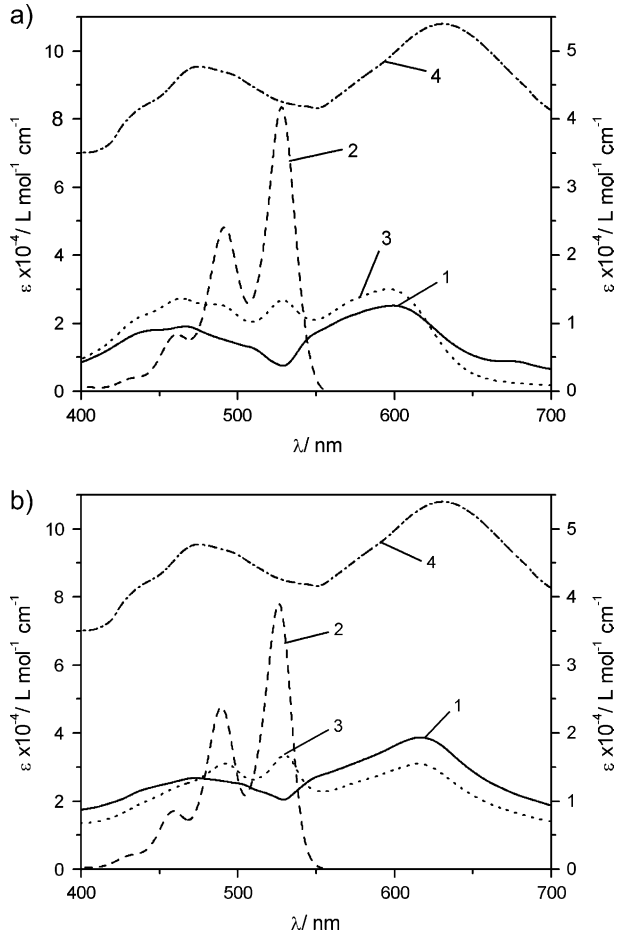

Fig. 5. Absorption spectra of diphenethylimide **1c** in (a) DMSO and (b) $CHCl_3$. Calculated dimer (1, solid line, scale on the right axis), calculated monomer (2, dashed line, scale on the left axis), concentrated solution (1.2×10^{-4} mol L^{-1} in DMSO and 1.7×10^{-4} mol L^{-1} in $CHCl_3$, 3, dotted line, scale on the right axis) absorption spectra and absorption spectrum of **1c** dispersed in a polyvinylbutyral film (4, dashed-dotted line, scale in arb.u.).

The ease of aggregation, which manifests itself as larger values of K, and the bathochromic shift of the longest wavelength maximum of the dimer, increases in the sequence **1a** < **1b** < **1c**. The intermolecular interaction strength in the solid-state increases in the same order [9,10]; **1c** corresponds to strong, while **1b** and **1a** correspond to medium and weak intermolecular interactions, respectively. This interaction manifests itself as a bathochromic shift in the absorption spectra of pigments dispersed in the polymeric film (555, 579, and 631 nm for **1a**, **1b**, and **1c**, respectively, as may be seen in Figs. 3–5).

Investigated 3,4,9,10-perylenetetracarboxylic acid diimides **1a–c** were used in photoreceptors as charge-generating materials. 3,4,9,10-Perylenetetracarboxylic acid bisbenzimidazole **2**, which exhibits very poor solubility for absorption spectra measurements, might also be used as an effective charge-generating material.

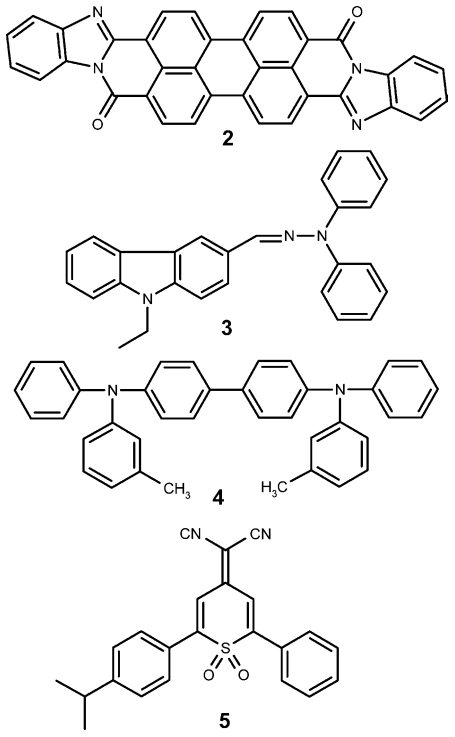

Fig. 6. Chemical structures of the materials used: 3,4,9,10-perylenetetracarboxylic acid bisbenzimidazole (**2**), ELA3011 (**3**), ELA4021 (**4**), and ST-917 (**5**).

The chemical structures of bisbenzimidazole **2** and used charge-transporting materials are presented in Fig. 6. The composition of prepared photoreceptors and measured xerographic characteristics are summarized in Table 2.

Since bisbenzimidazole **2** seems to be the one of most promising charge-generating materials, these photoreceptors were investigated in more detail. Dual-layered photoreceptors incorporating charge-transporting layers with hydrazone **3**, as well as with arylamine **4**, showed quite similar photosensitivity and its spectral dependence did not vary significantly. Spectral dependences of the photosensitivity for dual-layered photoreceptors with hole transport materials **3** (Table 2, entry 3) and **4** (Table 2, entry 4) are presented in Fig. 7. The spectral dependence of photosensitivity for a single-layered photoreceptor with bisbenzimidazole **2** is also shown (Table 2, entry 1). Unfortunately, the single-layered photoreceptor was approximately two times less sensitive as compared to the dual-layered system. The absorption spectrum of bisbenzimidazole **2** dispersed in polyvinylbutyral matrix is also presented in Fig. 7 for comparison.

According to the information, previously reported in patents, some additives, for instance, phthalocyanines [18,19] or electron donating dopants such as triarylamines [20,21], may significantly increase the photogeneration efficiency of perylene pigments. Therefore,

Table 2
Prepared photoreceptor configurations and their xerographic properties

Entry	Photoreceptor configuration	$t_{1/2}$ (s)	λ (nm)	$S_{1/2}$ ($m^2 J^{-1}$)	U_r (V)
1	[MKM] + [**2** + PVB + ELA3011 + ST-917]	40	600	45	27
2	[**2** + PVB] + [ELA3011 + PVB]	130		57	11
3	[MKM] + [**2** + PVB] + [ELA3011 + PVB]	62		98	10
4	[**2** + PVB] + [ELA4021 + PC]	>180		114	14
5	[MKM] + [**2** + PVB] + [ELA4021 + PC]	87		114	17
6	[**2** + 0.5% ELA4021 + PVB] + [ELA4021 + PC]	>180		102	20
7	[MKM] + [**2** + 0.5% ELA4021 + PVB] + [ELA4021 + PC]	122		100	26
8	[**2** + 1% ELA4021 + PVB] + [ELA4021 + PC]	>180		95	18
9	[MKM] + [**2** + 1% ELA4021 + PVB] + [ELA4021 + PC]	115		135	17
10	[MKM] + [**1a** + PVB + ELA3011 + ST-917]	29	480	<10	–
11	[**1a** + PVB] + [ELA3011 + PVB]	57		<10	–
12	[**1a** + PVB] + [ELA4021 + PC]	>180		<10	–
13	[MKM] + [**1b** + PVB + ELA3011 + ST-917]	17	600	<10	–
14	[**1b** + PVB] + [ELA3011 + PVB]	7.5		56	30
15	[**1b** + PVB] + [ELA4021 + PC]	33		13	23
16	[MKM] + [**1c** + PVB + ELA3011 + ST-917]	6	640	15	18
17	[**1c** + PVB] + [ELA3011 + PVB]	>180		63	11
18	[**1c** + PVB] + [ELA4021 + PC]	>180		19	10

$t_{1/2}$ – Potential dark half-decay time, $S_{1/2}$ – photosensitivity at the wavelength λ, U_r – residual potential.

dual-layered photoreceptors with triarylamine **4**-doped charge-generating layers (Table 2, entries 6–9) were prepared. However, the desired effect was not observed. Since the hole transporting material sensitize the photogeneration process at the charge-generating and charge-transporting layers interface [1,22], it seems that 1 mol% of amine **4** introduced into the charge generation layer did not significantly alter the photosensitivity due to a very large surface area of small pigment crystals (or aggregates) and very small amount of the introduced sensitizing agent. Incompatibility of polyvinylbutyral, used as a binder, and amine **4** does not allow to introduce a larger amount of the sensitizer into the charge-generating layer.

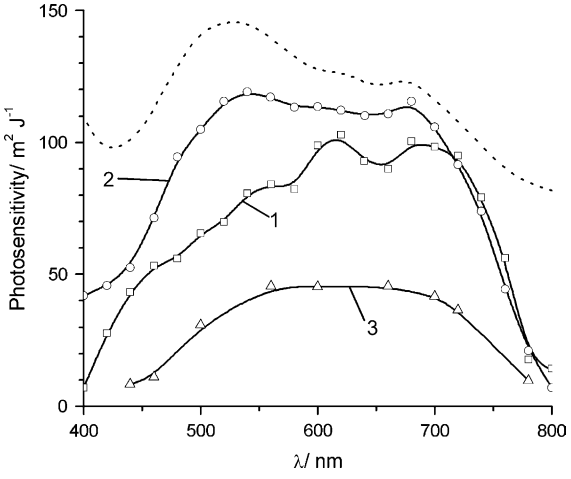

Fig. 7. Photosensitivity wavelength dependencies of photoreceptors containing 3,4,9,10-perylenetetracarboxylic acid bisbenzimidazole **2**. 1 – The dual-layered photoreceptor with a hydrazone **3** charge-transporting layer, 2 – the dual-layered photoreceptor with an arylamine **4** charge-transporting layer, 3 – the single-layered photoreceptor. The absorption spectrum of bisbenzimidazole **2** dispersed in a polyvinylbutyral film (dotted line) is presented for comparison.

The influence of the MKM charge blocking sublayer on the xerographic properties of dual-layered photoreceptors was also investigated (Table 2, entries 3, 5, 7 and 9 with MKM, entries 2, 4, 6 and 8 without the MKM layer). Though in two cases the greater photosensitivity of layers with a charge blocking sublayer was observed, faster dark decay ($t_{1/2}$ = 62–122 s as opposed to $t_{1/2}$ > 130 s for layers without MKM) was obtained in all the four cases. Besides, the charge generation layers coated directly onto the Al substrate were more homogeneous and possessed a smaller amount of defects, which could be evaluated even visually. For this reason, double-layered photoreceptors without charge blocking sublayers were used in the case of perylene compounds **1a**–**c**.

Photosensitivities of dual-layered photoreceptors containing diimides **1b** and **1c** were 55 and 63 $m^2 J^{-1}$, respectively, when hydrazone **3** was used as a charge-transporting material (Table 2, entries 14 and 17). Meanwhile, photosensitivities were much smaller with triarylamine **4** (Table 2, entries 15 and 18). The photosensitivity of single-layered photoreceptors (Table 2, entries 13 and 16), as in the case of bisbenzimidazole **2**, was also much smaller. Although they possessed sufficient photosensitivity, photoreceptors with dibenzylimide **1b** showed rather a fast dark decay ($t_{1/2}$ was about 7.5 s). Spectral dependences of the photosensitivity as well as absorption spectra of diimides **1b** and **1c** dispersed in polyvinylbutyral film are presented in Fig. 8.

Diphenylimide **1a** did not show sufficient photosensitivity. A weak intermolecular interaction between the

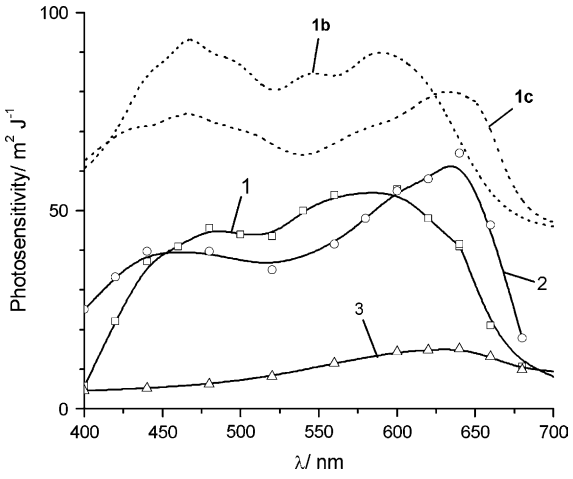

Fig. 8. Photosensitivity wavelength dependencies of photoreceptors containing 3,4,9,10-perylenetetracarboxylic acid diimides **1b** and **1c**. 1 – The dual-layered photoreceptor with **1b** and hydrazone **3** charge-transporting layer, 2 – the dual-layered photoreceptor with **1c** and hydrazone **3** charge-transporting layer, 3 – the single-layered photoreceptor with **1c**. Absorption spectra of diimides **1b** and **1c** dispersed in a polyvinylbutyral film (dotted lines) are presented for comparison.

neighboring pigment molecules in the solid polymeric matrix may be the reason of such behavior [1,23].

4. Conclusions

Perylenetetracarboxylic acid diimides **1a–c** undergo aggregation to form dimers in chloroform and DMSO solutions at higher concentrations. This manifests itself as a decrease in the monomer absorbance at about 530 nm and an appearance of a new broad absorption band in the 560–610 nm spectral region. Pure monomer and pure dimer spectra were calculated from the set of pigment absorption spectra at various solution concentrations. Calculated monomer spectra in all the cases were very similar to those of dilute solutions and are formed by the $\pi-\pi^*$ transition band with a characteristic vibronic structure. Dimer bands in the evaluated dimer spectra are split into two peaks: one at the longer, and another one at shorter wavelengths relative to a monomeric lowest energy transition. The calculated dimer spectra are quite similar to the absorption spectra of the pigment dispersed in a polyvinylbutyral film, but concentrated solution spectra in DMSO resemble the solid-state absorption spectra much better. The aggregation process is more favorable in DMSO than in chloroform. This is in line with obtained greater values of K in DMSO than in chloroform for all investigated pigments **1a–c**. This indicates that the increase in polarity during the aggregation (DMSO is much more polar solvent than chloroform) may be caused by the formation of charge transfer complexes.

Photosensitivity of the single-layered photoreceptor with perylenetetracarboxylic acid bisbenzimidazole **2** was about 50 m^2 J^{-1} while the dual-layered photoreceptors were 2–3 times more sensitive. Doping the charge generation layer with up to 1 mol% of triarylamine **4** practically does not have any effect on the system's photosensitivity. The possible reason is that a hole transport molecule acts as a sensitizer at the charge-generating and charge-transporting layer interface and a small concentration of the dopant in the charge-generating layer bulk does not significantly alter the photogeneration efficiency. The dual-layered photoreceptors with diimides **1b** and **1c** and hydrazone **3** CTL were 3–4 times more sensitive than ones employing triarylamine **4** CTL.

Acknowledgments

This work was supported by the Lithuanian State Science and Studies Foundation.

Appendix 1. Calculation of monomer and dimer absorption spectra

The detailed description of the calculation of pure monomer and dimer absorption spectra making use of different concentration solution absorption spectra is presented here. The calculation example presented here is for the dibenzylimide **1b** solutions in DMSO.

The expressions of the equilibrium constant K, monomer and dimer concentrations [M] and [D] as well as fraction of the monomer f_m were presented earlier in Eqs. (1)–(3). It follows from these equations that

$$\log(1-f_m)c = n\log(f_m c) + \log K + \log n. \quad (4)$$

It is clear from Eq. (4) that dependence of $\log(1-f_m)c$ vs. $\log(f_m c)$ is linear. It would be possible to calculate n and K from this dependence if the value of f_m was known.

Having a set of spectra obtained at different concentrations, f_m values may be determined in the following way. Fig. 9 shows a plot of the ratio of the extinction coefficient of the pigment **1b** in DMSO measured at 529 nm to that at 547 nm ($\varepsilon_{529}/\varepsilon_{547}$) as a function of $\log c$. The wavelength at 529 nm was selected because the change in ε value for the conversion of the monomer to the dimer was highest namely at 529 nm (there is a monomer absorption peak, and its intensity considerably decreases increasing the concentration of the solution). The division of ε_{529} by the isosbestic value at ε_{547} reduces the effects of non-systematic errors in the values of c of the samples. The ratio $\varepsilon_{529}/\varepsilon_{547}$ is related to f_m according to

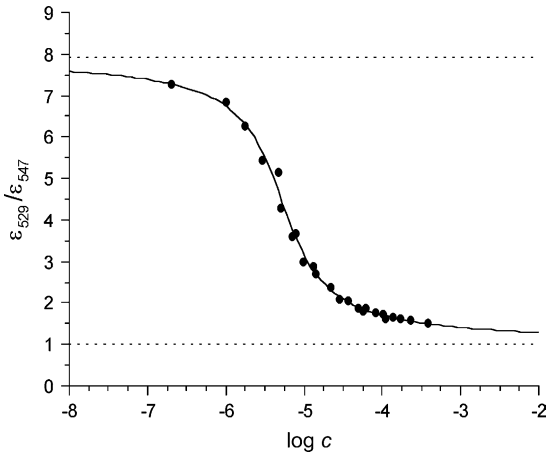

Fig. 9. Plot of $(\varepsilon_{529}/\varepsilon_{547})$ as a function of $\log c$ for **1b** solutions in DMSO. Points correspond to experimental data, the solid lines show a fit using an arctangent function, dotted lines show limiting values.

$$1-f_m=\frac{(\varepsilon_{529}/\varepsilon_{547})_{max}-(\varepsilon_{529}/\varepsilon_{547})}{(\varepsilon_{529}/\varepsilon_{547})_{max}-(\varepsilon_{529}/\varepsilon_{547})_{min}}. \quad (5)$$

Maximum and minimum values of $\varepsilon_{529}/\varepsilon_{547}$ are obtained by the extrapolation of the plot to the limiting value of c for the pure monomer ($f_m = 1$, $c = 0$) and for the pure dimer ($f_m = 0$, $c = \infty$), respectively. Based on the plot in Fig. 9, the limiting values of $(\varepsilon_{529}/\varepsilon_{547})_{max} \approx 8$ and $(\varepsilon_{529}/\varepsilon_{547})_{min} \approx 1$ were obtained. The analytical arctangent function $y = a + b$ arctg $(c + dx)$ fits experimental data well ($a = 4.46$, $b = -2.20$, $c = 12.56$, $d = 2.38$, $r = 0.997$), giving $(\varepsilon_{529}/\varepsilon_{547})_{max} = 7.92$ and $(\varepsilon_{529}/\varepsilon_{547})_{min} = 1.01$. f_m values were calculated using these obtained values and a plot of $\log(1-f_m)c$ vs. $\log(f_m c)$ obtained is presented in Fig. 10. A fit with a linear function gave the following results: $y = a + bx$, $b = n = 2.21$, $a = \log K + \log n = 6.94$, $r = 0.981$, $\log K = 6.60$.

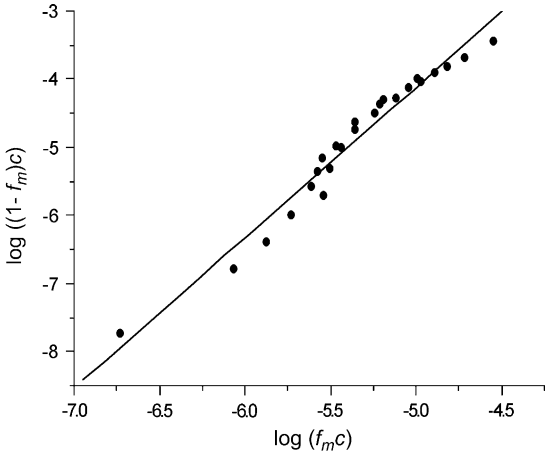

Fig. 10. Plot of $\log(1-f_m)c$ vs. $\log(f_m c)$ of **1b** solutions in DMSO.

The obtained value of $n = 2.21$ corresponds to the situation when a dimer formation is more preferable (where n must be 2). The possible reasons for the difference may be caused by inadequacy of the selected analytical arctangent function to reality, some experimental errors related to very low pigment concentrations and very low signals, or by solvation effects. But the most preferable reason is a formation of higher order aggregates, maybe even colloidal particles, especially at very high pigment concentrations.

Assuming that extinction coefficients are additive, the overall ε of the sample may be expressed as

$$\varepsilon = f_m\varepsilon_m + \frac{(1-f_m)\varepsilon_d}{2}, \quad (6)$$

where ε_m and ε_d are extinction coefficient values for the pure monomer and dimer, respectively. The magnitude of ε_d is divided by 2 since the dimer concentration is half as much as compared to the same concentration of the monomer. Applying Eq. (6), it is possible to calculate absorption spectra of the pure monomer and the pure dimer (i.e., the wavelength dependence of ε_m and ε_d) from two spectra with different solution concentrations using the f_m value derived from Eq. (5). For this case several points are taken from Fig. 10, monomer and dimer spectra from different point pairs were calculated and, finally, averaged. Only points best fitting the linear dependence in Fig. 10 were used in the calculation in order to minimize experimental errors.

References

[1] Law KY. Organic photoconductive materials: recent trends and developments. Chem Rev 1993;93:449–86.
[2] Borsenberger PM, Weiss DS. Organic photoreceptors for xerography. New York: Marcel Dekker; 1998.
[3] Kalinowski J, Di Marco P, Camaioni N, Fattori V, Stampor W, Duff J. Injection-controlled and volume-controlled electroluminescence in organic light-emitting diodes. Synth Met 1996;76:77–83.
[4] Kalinowski J, Di Marco P, Fattori V, Giulietti L, Cocchi M. Voltage-induced evolution of emission spectra in organic light-emitting diodes. J Appl Phys 1998;83:4242–8.
[5] Horowitz G. Organic field-effect transistors. Adv Mater 1998;10:365–77.
[6] Woehrle D, Meissner D. Organic solar cells. Adv Mater 1991;3:129–38.
[7] Graser F, Haedicke E. Kristallstruktur und farbe bei perylen-3,4:9,10-bis(dicarboximid)-pigmenten. Liebigs Ann Chem 1980;1994–2011.
[8] Graser F, Haedicke E. Kristallstruktur und farbe bei perylen-3,4:9,10-bis(dicarboximid)-pigmenten 2. Liebigs Ann Chem 1984;483–94.
[9] Klebe G, Graser F, Haedicke E, Berndt J. Crystallochromy as a solid-state effect: correlation of molecular conformation, crystal packing and colour in perylene-3,4,9,10-bis(dicarboximide) pigments. Acta Crystallogr 1989;B45:69–77.
[10] Haedicke E, Graser F. Structures of eleven perylene-3,4,9,10-bis(dicarboximide) pigments. Acta Crystallogr 1986;C42:189–95.

[11] Wuerthner F, Thalacker C, Sautter A. Hierarchical organization of functional perylene chromophores to mesoscopic superstructures by hydrogen bonding and π–π interactions. Adv Mater 1999;11:754–8.
[12] Ebeid EM, El-Daly SA, Langhals H. Emission characteristics and photostability of *N*,*N*′-bis(2,5-di-*tert*-butylphenyl)-3,4:9,10-perylenebis(dicarboximide). J Phys Chem 1988;92:4565–8.
[13] Mazur G, Petelenz P. Charge transfer excitons in perylenetetracarboxylic dianhydride microelectrostatic calculations. Chem Phys Lett 2000;324:161–5.
[14] Sapagovas VJ, Kadziauskas P, Undzenas A, Purlys R. Synthesis and optical properties of 3,4,9,10-perylenetetracarboxylic acid derivatives. Environ Chem Phys 2001;23:30–7.
[15] Ford WE. Photochemistry of 3,4,9,10-perylenetetracarboxylic dianhydride dyes: visible absorption and fluorescence of the di(glycyl)imide derivative monomer and dimer in basic aqueous solutions. J Photochem 1987;37:189–204.
[16] Bergmann K, O'Konski CT. A spectroscopic study of methylene blue monomer, dimer and complexes with montmorillonite. J Phys Chem 1963;67:2169–77.
[17] West W, Pearce S. The dimeric state of cyanine dyes. J Phys Chem 1965;69:1894–903.
[18] Mishra S, Horgan AM, Carmichael KM, Sullivan DP, Nonkes S. Photoreceptor with adjustable charge generation section. US patent 6,350,550; 2002.
[19] Mishra S, Horgan AM, Carmichael KM, Nonkes S. Photoreceptor with layered charge generation section. US patent 6,376,141; 2002.
[20] Yuh HJ, Chambers JS, Pai DM, Yanus JF. Photoreceptor with donor molecule in charge generating layer. US patent 5,863,686; 1999.
[21] Yanus JE, Pai DM, Fuller TJ, Prosser DJ, Vandusen SM. Generator layer sensitization through transport layer doping. US patent 6,063,533; 2000.
[22] Popovic ZD, Hor AM, Loutfy RO. A study of carrier generation mechanism in benzimidazole perylene/tetraphenyldiamine thin film structures. Chem Phys 1988;127:451–7.
[23] Loutfy RO, Hor AM, Kazmaier P, Tam M. Layered organic photoconductive devices incorporating *N*,*N*′-disubstituted diimide and bisarylimidazole derivatives of perylene-3,4,9,10-tetracarboxylic acid. J Imaging Sci 1989;33:151–9.